The Prognosis and Immune Microenvironment Related Factor Interleukin-23 in Clear Cell Renal Cell Carcinoma: A Radiological Investigation

Lianghong Jiao[1], Xiaofeng Wang[1], Yibo Ying[1], Kewei Yang[1*]

1 Department of Radiology, Ningbo Urology and Nephrology Hospital, Ningbo, China

Correspondence to: Kewei Yang. Department of Radiology, Ningbo Urology and Nephrology Hospital, Ningbo 315000, China.

Email: syzdh_keweiyang@hotmail.com

Key words: clear cell renal cell carcinoma; interleukin-23; tumor microenvironment; computed tomography; radiomics

ABSTRACT

Purpose: To explore the ccRCC clinical and immune characteristics correlated with IL-23 expression level and build pre-operative prediction models based on contrast CT scans.

Materials and Methods: The study included the cancer genome atlas kidney renal clear cell carcinoma cases to build a bioinformatics cohort. The cases with qualified contrast CT images were selected as radiographic and radiomics cohort. The IL-23 expression level groups were defined by median-based thresholding. The clinical characteristics were compared between groups. The impacts of IL-23 on immune microenvironment composition were measured via the CIBERSORT. Two radiologists evaluated the pre-operative contrast CT images. The radiomics features were automatically extracted. IL-23 group-specific radiographic and radiomics features were collected and used for prediction model establishment via Orange Data Mining Toolbox. $P < 0.05$ was set as statistically significant.

Results: For total, 530 ccRCC cases were included. The IL-23 group was significantly associated with survival, histologic grade, AJCC tumor stage, AJCC cancer stage, and plasma calcium level. Except for Treg and other T cells, IL-23 showed correlation with NK cell, mast cell, monocyte infiltration. Axial length was the only significant radiographic measurement between IL-23 groups. The radiomics features established an IL-23 group prediction model with the highest 10-fold cross-verification AUC of 0.842.

Conclusion: The clear cell renal cell carcinoma IL-23 expression level had prognosis and immune microenvironment correlation and could be predicted by pre-operative radiomics features.

INTRODUCTION

The clear cell renal cell carcinoma (ccRCC), as one of the most common kidney cancers, still has increasing incidence and dismal advanced stage prognosis until now, which urgently calls for novel therapies.[1] Except for the previous breakthrough of tyrosine kinase inhibitors,[2] novel immune therapies include anti-programmed cell death 1/ligand 1 (PD-1/PD-L1) in recent showed encouraging result in clinical trials.[3] However, the non-satisfied response to immune therapies immediately became the next clinical application barrier.[4] Previous studies suggested tumor related cells could contribute to response variation of immune therapies.[5] Moreover, both the prospective clinical trial evidence and retrospective analysis supported the tumor microenvironment (TME) significant contribution in immune therapy resistance.[6] A detailed understanding of TME related immune regulation mechanisms is thus become the key to ccRCC treatment development.

The Interleukin-23 (IL-23) is a member of the interleukin-12 cytokine family that is secreted by antigen-presenting cells like macrophage cells.[7] In 2018, Fu et al. reported the high expression of tumor-associated macrophage secreted IL-23 in ccRCC could enhance the immunosuppressive function of Treg cells based on in-vivo and in-vitro evidence.[8] But the IL-23's impact on other immune cells remains unclear. A detailed description of IL-23 related ccRCC clinical characteristics were not yet established. This situation undoubtedly slowed down the targeted IL-23 examination and immunotherapy development.

The imaging-based classification of ccRCC clinical and genetic status has gained considerable

attention in recent years.[9] The radiogenomics analysis matches the ccRCC major mutations and genetic clusters with radiographic evaluation result,[10,11] which was manual and thus clinically meaningful. The differentiative radiological feature combinations could be summarized as phenotypes and directly help the clinical practice. The radiomics analysis extracts quantitative image features and make ccRCC clinical classifications.[12] Taken together, the radiogenomics and radiomics workflows have shown the potential ability in ccRCC genetic subtype prediction. However, the treatment-assistant IL-23 expression status pre-operative prediction based on these radiological methods was still not available until now.

In this one-stop study, we aimed to comprehensively describe the clinical and immune relevance of IL-23 expression level. We also assumed that by using the radiographic and radiomics methods, the IL-23 specific radiological phenotype and prediction model could be established.

MATERIALS and METHODS

Cohorts and ethics

This study's patient list was retrieved from The Cancer Genome Atlas Kidney Renal Clear Cell Carcinoma (TCGA-KIRC) data collection (https://portal.gdc.cancer.gov/projects/TCGA-KIRC). Initially, the study included the patients with available clinical and transcriptome profiling data to build clinical and bioinformatics analysis cohort (TCGA-Bioinfo). The patients with single tumor and pre-operative contrast CT imaging data available on The Cancer Imaging Archive (https://www.cancerimagingarchive.net/) were selected as a manual radiographic evaluation cohort (TCGA-Radiographic).[13] Finally, a radiomics analysis cohort (TCGA-Radiomics) was

subsetted from the TCGA-Radiographic cohort using followed exclusion criteria: 1. The cases with image artifacts. 2. The cases with non-routine CT scan protocols including tube voltage > 150 kV, slice thickness > 5 mm, and pixel spacing > 1 mm. 3. The images that may cause significant cohort heterogeneity due to phase selection or small center scale. 4. The ccRCC lesion could not be segmented due to uncertain margin. Since all the patients and responsible clinical, radiological, genetic data were obtained from the public available and anonymized TCGA database, the informed consent and registration were waived from the institutional review board.

IL-23 group clinical and transcriptome bioinformatics analysis

The RNA-Seq raw count data from the Genomic Data Commons portal (https://portal.gdc.cancer.gov/projects/TCGA-KIRC) was used to build IL-23 expression level groups (high expression and low expression) by median-based thresholding. In clinical analysis, the overall survival, diagnosis age, histologic grade, American Joint Committee on Cancer Clinical (AJCC) staging result, hemoglobin level, platelet count, calcium level, and white blood cell status were retrieved. The cases without target item data would be removed in particular statistical tests. In bioinformatics analysis, the R package limma (version 3.40.2) with the threshold of adjusted $P < 0.05$ and the absolute log2(fold change) > 1 was used to perform mRNA differential expression study. The resulted gene list was further annotated with Gene Ontology (GO) and Kyoto Encyclopedia of Genes and Genomes (KEGG), by using the R package ClusterProfiler (version 3.18.0). To explore the impact of IL-23 expression level on immune cell spectrum, the CIBERSORT calculated immune cell percentage data of TCGA cohort were downloaded from http://timer.cistrome.org/. CIBERSORT is a deconvolution method that calculates the cell percentage of interest based on mRNA expression matrix input

based on gene signature. We also compared the reported immune checkpoint-related genes' expression level between IL-23 groups and control tissues. The control tissues include 72 peritumoral samples from TCGA and 89 healthy samples from Genotype-Tissue Expression (GTEx).

CT equipment and protocol

The study included CT scan images from four American TCGA tissue source sites. The scanner models include the Lightspeed series (GE Healthcare, United States) and the Sensation series (Siemens Healthineers, Germany). The usual scan protocol was as follows: Scan type: Helical; kVp = 120; Slice thickness: 2.5 mm. It should be noticed that the the Cancer Imaging Archive (TCIA) images did not contain detailed multiphase imaging protocol information, which was determined by the previous reported cortex and medulla enhancement pattern.[14]

Radiographic evaluation

Two board-certified abdominal radiologists independently evaluated the radiographic features of the TCGA-Radiographic cohort. The evaluation items include lesion side, axial length, margin status (well-defined or ill-defined), signal characteristic (solid or cyst), necrosis status (with or without), calcification status (with or without), and grow pattern (entirely endophytic, < 50% exophytic, ≥ 50% exophytic). Two radiologists could voluntarily browse all the available studies while being blind to clinical information. The radiographic evaluation procedure in this study was verified by intraclass correlation index (ICC).

Image pre-processing and Tumor region of interest segmentation

The 1 mm3 voxel resampling as normalization method and wavelet transformation as image augmentation method was applied. The tumor region of interest (ROI) was primarily segmented by one of the radiologists and revised by another. The radiologists could browse all the available

pre-operative imaging studies while being blinded to clinical information. If the intersection voxels of original and revised ROI were less than 90% of the original ROI, two radiologists would discuss and decide the final ROI. The intersection voxel calculation was executed by using FMRIB Software Library (version 6.0.1).

Radiomics feature extraction and filtration

The radiomics features include shape, first order, glcm, gldm, glrlm, glszm, and ngtdm were extracted using Pyradiomics (version 3.0.1, https://github.com/AIM-Harvard/pyradiomics). To reduce the redundancy, highly correlated (spearman $r > 0.90$) and linear combined features were filtrated by using R (version 4.0.3) and R package caret (version 6.0-86, https://cran.r-project.org/web/packages/caret/index.html).[15]

Machine learning model establishment and evaluation

The study used Orange Data Mining Tool (version 3.27) to execute feature selection and establish the IL-23 status prediction model. The TCGA-radiomics cohort was separated as a training set and validation set in a 10-fold fashion. After the information entropy gain-based feature selection, the classical machine learning algorithms (support vector machine; random forest; k-nearest neighbors; neural network) was used to train the prediction model. The overall AUC, accuracy, sensitivity, and specificity were reported to represent the model performance.

Statistics and visualization

The Kolmogorov-Smirnov test was first performed on continuous variables to confirm normal distribution, and the responsible parametric and non-parametric test was performed. For categorical variables, a chi-squared test and conditional corrections were performed. These statistical analyses were executed by using SPSS (version 22.0). The Spearman correlation test was performed by using R (version 4.0.3). The $P < 0.05$ was set as statistically significant. For

Kaplan-Meier survival analysis, R package survival (version 3.2-7, https://cran.r-project.org/web/packages/survival/index.html) and survminer (version 0.4.9). The heatmap, dot plot, half-violin plot, ROC curve, and Venn diagram were plotted via Hiplot (https://hiplot.com.cn/).

RESULTS

Clinical characteristics

The study included 530 ccRCC cases from the TCGA database as TCGA-Bioinfo cohort, in which 130 and 45 cases were selected as TCGA-Radiographic and TCGA-Radiomics cohort. The clinical characteristics of all three cohorts were summarized in Table 1. The distribution of IL-23 expression status, age at diagnosis, histological grade, and AJCC stage between TCGA-Radiographic and TGCA-Radiomics cohort was not significantly different ($P > 0.05$), which supported the consistency of manual and automatic radiological analysis in this study. The histological grade composition was, however, different in all cohorts compare. The benefit of IL-23 low expression was confirmed in survival analysis ($P < 0.001$). A higher-grade preference, worse AJCC stage presentation (except for lymph node stage), and more elevated serum calcium level were observed (see Figure 1) in IL-23 high expression group. The large portion of data point missing for AJCC lymph node staging should be noticed.

IL-23 related pathway enrichment analysis

The IL-23 group-related differential expression of mRNAs was visualized as a volcano plot and annotated by GO and KEGG pathway enrichment methods, which were summarized in supplementary file 1. The broad immune cell differentiation, activation, adhesion, and response role of IL-23 in physiological and disease-related conditions could be observed.

Roles of IL-23 in tumor immune microenvironment and response

The CIBERSORT-deconvoluted tumor immune microenvironment composition was plotted in Figure 2. Except for several T lymphocytes, immune cells include monocyte, and mast cell activated, NK cell activated also showed IL-23 consistent clustering tendency (P = .00246; P = .000578; P = .0269). The immune checkpoints related gene expression also showed correlation with ccRCC and IL-23 expression (the results were summarized in supplementary file 1).

Radiographic evaluation results

In the TCGA-Radiographic cohort, two radiologists evaluated the pre-operative contrast CT scans from seven aspects: lesion side, axial length, margin, necrosis, signal, calcification, and growing pattern. However, the necrosis evaluation was excluded due to nonideal ICC (< 0.8). The axial length was significantly different between IL-23 groups (P < 0.001, Figure 3). The remaining four radiographic evaluation aspects were shown in supplementary file 1.

Radiomics analysis and machine learning model training

A total of 851 radiomics features were extracted from pre-operative contrast CT scan images of 45 TCGA-Radiomics ccRCC cases. After dimension reduction, 45 radiomics features were kept and plotted in Figure 4A. Since the spearman correlation test still showed considerable redundancy in kept features (summarized in supplementary file 1). The information entropy gain-based feature selection was applied before model training, which was summarized in Table 2. The Random Forest method achieved the best performance with the highest 10-fold cross-validation AUC of 0.842 (see Figure 4B and Table 3). The model performance information was

summarized in Table 4. The established models have higher prediction ability in recognition of IL-23 high expression cases than low expression cases. The same information entropy gain method was applied to get a grade and survival-related radiomics features to distinguish if such prediction equals grade or survival prediction. The logical relationships between these three groups of features were summarized in supplementary file 1, in which seven radiomics features had prediction ability specific to IL-23 status only. All the generated IL-23 expression status prediction models and study protocols were available upon E-mail request.

DISCUSSION

Due to the adjuvant therapy insensitivity and supportive tumor pathogenesis findings, the immune therapy of ccRCC has gained significant attention since the last century.[16] Marked by introducing interferon-alpha (IFN-α) and interleukin-2 (IL-2), early-stage immune therapy brought encouraging prognosis improvement while accompanied by non-negligible toxicity.[17,18]To overcome these drawbacks caused by systemic pharmacological reaction, the current ccRCC immune therapy focuses on tumor local immune regulation. The immune-checkpoint inhibitors like PD-1 blocking antibody could normalize T-cell response in anti-tumor activity and has been proved to be effective in ccRCC.[19]Nevertheless, the regulatory T cells (Tregs) were later found to attenuate such tumor immune response via various mechanisms and became the next barrier.[20]In 2018, Fu et al. reported IL-23 secreted by tumor-infiltrating macrophages could activate Tregs and subsequently decrease T-cell mediated tumor cell killing.[8]Targeting the IL-23 thus became a promising option in ccRCC immune therapy enhancement. Moreover, the preclinical mouse study proved the role of IL-23 in glioma, lung metastases, and bladder cancer further described the research value of IL-23 in ccRCC. However, a detailed clinical and immune relevance study of IL-23 expression level was still rare.

The IL-23 specific radiological phenotype was not yet available for targeted screening. Our study re-confirmed the unfavorable survival, grade, and AJCC tumor staging role of the IL-23 high expression group ($P < 0.001$; $P < 0.001$; $P = .002$). We found the AJCC lymph node stage was not significantly different between IL-23 expression groups. The IL-23 high expression group has higher serum calcium level than the low expression group ($P = .048$). In bioinformatics analysis, the IL-23 expression group showed an impact on general immune cell function alteration. The monocyte and mast cell activated, NK cell activated showed IL-23 expression group-similar clustering tendency ($P = .00246$; $P = .000578$; $P = .0269$). In radiographic evaluation, the IL-23 high expression group was found to have a larger axial length than the low expression group. In radiomics analysis, we established an IL-23 expression group prediction model based on the pre-operative contrast CT radiomics features. The best 10-fold cross-validation AUC was 0.842 when using the Random Forest algorithm. The modeling radiomics features were different from survival or grade-prediction needed radiomics features.

The European Association of Urology renal cell cancer guidelines have comprehensively described the clinical decision making based on classical cancer staging tools include age, grade, size, AJCC primary tumor staging, and distant metastasis staging.[18]The regional lymph node staging contribution to the clinical decision, however, was not confirmative. The reasons could be the low positive rate and controversial prognosis correlation.[21]Our study also noticed a large portion of the cohort did not have lymph node staging information, resulting in an insignificant difference between IL-23 expression groups. Zhi et al. in 2020 reported the Surveillance, Epidemiology, and End Result database ccRCC cohort supported larger sized tumors had higher lymph node metastases risk.[22]In our study, we also found a larger axial length in the IL-23 high

expression group. Taken together, this insignificant difference between IL-23 and lymph node status would still need further study with available pathological information to verify. The classical ccRCC outcome-related blood markers include serum lactate dehydrogenase, hemoglobin, serum calcium level, platelets, and neutrophil count.[23]Interestingly, all included blood markers except serum calcium level showed an insignificant difference between IL-23 expression groups, which might reflect the unique IL-23 expression-related outcome alteration mechanism. In many bone-related autoimmune diseases include spondyloarthritis and osteoarthritis, the IL-23/17 axis was proven to play the central role as osteogenesis and osteoclastic activity regulator.[24]Vitamin D was also found to interact with immune check-point inhibitors in multiple disease.[25,26]Thus, the IL-23 expression level could theoretically cause the observed serum calcium level change and indirectly resulted in ccRCC immune evasion. Taken together, this clinical evidence found in our study showed the complex role that IL-23 might have in ccRCC.

The immune evasion mechanism of IL-23 reported by Fu et al. in 2018 focused on the T cells and macrophages.[8]Nevertheless, other immune cells were not detailed evaluated. Our study found monocyte and NK cell percentages were significantly different between IL-23 expression groups ($P < 0.05$). Consider the known macrophage-differentiation behavior of monocyte and the near gene expression pattern between T cells and NK cells.[27]The difference mentioned above could be associated with macrophage's IL-23 production and downstream immune evasion. Our study also showed mast cell percentage was significantly different between IL-23 expression groups. Although mast cells could respond to IL-23 stimulation and exogenously secrete IL-17, the IL-23 related infiltration difference has not been well studied. Nakano et al. in 2007

described mouse bone marrow–derived mast cells could produce IL-23 subunit, P40 protein.[28]However, the mast cell IL-23 production in that study was only partially supported due to the lack of an IL-23 ELISA system. This finding requires further exploration study. We also evaluated eight related transcripts. The general higher transcript expression confirmed the immunosuppressive role of IL-23.

The tumor treatment-naïve imaging scan has been recognized as a data bridge that connects the genetic background and clinical manifestations. Shinagare et al. in 2015 matched the pre-operative imaging radiological characteristics with ccRCC major mutations.[29]The results suggested tumor margin, calcification, growing pattern were related to BAP1 and MUC4 mutations, which showed the feasibility of image-gene analysis. Karlo et al. in 2014 reported CT radiographic features included tumor margin, nodular enhancement, vascularity appearance, renal vein invasion, and cystic tumor could help differentiate ccRCC mutation status.[11]In our study, the axial length was the only significant radiographic feature between IL-23 expression groups. Kocak et al. in 2019 reported the PBRM1 mutation status of ccRCC could be predicted via a machine learning-based radiomics model.[30]Our study also established IL-23 expression group prediction models based on radiomics features. The model used random forest achieved the highest 10-fold cross-verification AUC of 0.842. Seven of predictive radiomics features only worked for IL-23 expression prediction without grade or OS relation, which indicated the unique texture influence caused by IL-23 expression.

This study has several limitations. First, the TCGA cohort was retrospectively collected. Second, the study scale was limited due to the transcriptome profiling and pre-operative CT scan imaging data availability. However, consider the scarcity of imaging-sequencing paired data, this limitation was understandable. Third, the IL-23 radiological phenotype obtained in this study could be non-specific due to confounding factors like grade and survival group. However, as we have mentioned above, the predictive radiomics features of the IL-23 group were not perfectly overlapped with the grade or survival group. We also noticed the clinical characteristic analysis of included TCGA ccRCC cases could still be improved by joining of more local-center and other renal cancer data. Indeed, a further prospective, multicenter, multimodal study was expected to verify and explore more about the IL-23 related radiological phenotype.

CONCLUSION

Our study confirmed the role of IL-23 as a prognosis and immune microenvironment-related factor. The IL-23 high expression ccRCCs were radiologically characterized by larger axial length on preoperative contrast CT scan. The radiomics machine learning model could predict the IL-23 expression group and help pre-operative targeted examination.

ACKNOWLEDGEMENT

The results here are part based upon data generated by the TCGA Research Network: http://cancergenome.nih.gov/.

CONFLICT OF INTEREST

The authors report no conflict of interest.

REFERENCE

1. Bray F, Ferlay J, Soerjomataram I, Siegel RL, Torre LA, Jemal A. Global cancer statistics 2018: GLOBOCAN estimates of incidence and mortality worldwide for 36 cancers in 185 countries. CA Cancer J Clin. 2018;68:394-424.
2. Motzer RJ, Hutson TE, Tomczak P, et al. Overall survival and updated results for sunitinib compared with interferon alfa in patients with metastatic renal cell carcinoma. J Clin Oncol. 2009;27:3584.
3. Motzer RJ, Escudier B, McDermott DF, et al. Nivolumab versus everolimus in advanced renal-cell carcinoma. N Engl J Med. 2015;373:1803-13.
4. Rini BI, Plimack ER, Stus V, et al. Pembrolizumab plus axitinib versus sunitinib for advanced renal-cell carcinoma. N Engl J Med. 2019;380:1116-27.
5. Motzer RJ, Rini BI, McDermott DF, et al. Nivolumab for metastatic renal cell carcinoma: results of a randomized phase II trial. J Clin Oncol. 2015;33:1430.
6. McDermott DF, Huseni MA, Atkins MB, et al. Clinical activity and molecular correlates of response to atezolizumab alone or in combination with bevacizumab versus sunitinib in renal cell carcinoma. Nat Med. 2018;24:749-57.
7. Gaffen SL, Jain R, Garg AV, Cua DJ. The IL-23–IL-17 immune axis: from mechanisms to therapeutic testing. Nat Rev Immunol. 2014;14:585-600.
8. Fu Q, Xu L, Wang Y, et al. Tumor-associated macrophage-derived interleukin-23 interlinks kidney cancer glutamine addiction with immune evasion. Eur Urol. 2019;75:752-63.
9. Nie P, Yang G, Wang Z, et al. A CT-based radiomics nomogram for differentiation of renal angiomyolipoma without visible fat from homogeneous clear cell renal cell carcinoma. Eur Radiol. 2020;30:1274-84.
10. Jamshidi N, Jonasch E, Zapala M, et al. The radiogenomic risk score: construction of a prognostic quantitative, noninvasive image-based molecular assay for renal cell carcinoma. Radiology. 2015;277:114-23.
11. Karlo CA, Di Paolo PL, Chaim J, et al. Radiogenomics of clear cell renal cell carcinoma: associations between CT imaging features and mutations. Radiology. 2014;270:464-71.
12. Stanzione A, Ricciardi C, Cuocolo R, et al. MRI radiomics for the prediction of Fuhrman grade in clear cell renal cell carcinoma: A machine learning exploratory study. J Digit Imaging. 2020;33:879-87.
13. Clark K, Vendt B, Smith K, et al. The Cancer Imaging Archive (TCIA): maintaining and operating a public information repository. J Digit Imaging. 2013;26:1045-57.
14. Cohan RH, Sherman LS, Korobkin M, Bass JC, Francis IR. Renal masses: assessment of corticomedullary-phase and nephrographic-phase CT scans. Radiology. 1995;196:445-51.
15. Ihaka R, Gentleman R. R: a language for data analysis and graphics. J Comput Graph Stat. 1996;5:299-314.
16. Jonasch E, Walker CL, Rathmell WK. Clear cell renal cell carcinoma ontogeny and mechanisms of lethality. Nat Rev Nephrol. 2020;17:245-61.
17. McDermott D, Ghebremichael M, Signoretti S, et al. The high-dose aldesleukin (HD IL-2)"SELECT" trial in patients with metastatic renal cell carcinoma (mRCC). J Clin Oncol. 2010;28:4514.
18. Ljungberg B, Bensalah K, Canfield S, et al. EAU guidelines on renal cell carcinoma: 2014 update. Eur Urol. 2015;67:913-24.
19. Mazza C, Escudier B, Albiges L. Nivolumab in renal cell carcinoma: latest evidence and clinical potential. Ther Adv Med Oncol. 2017;9:171-81.

20. González-Navajas JM, Fan DD, Yang S, et al. The impact of Tregs on the anticancer immunity and the efficacy of immune checkpoint inhibitor therapies. Front Immunol. 2021;12:416.
21. Blom JH, van Poppel H, Maréchal JM, et al. Radical nephrectomy with and without lymph-node dissection: final results of European Organization for Research and Treatment of Cancer (EORTC) randomized phase 3 trial 30881. Eur Urol. 2009;55:28-34.
22. Zhi Y, Li X, Qi F, Hu X, Xu W. Association of Tumor Size with Risk of Lymph Node Metastasis in Clear Cell Renal Cell Carcinoma: A Population-Based Study. J Oncol. 2020;2020:e8887782.
23. Heng DY, Xie W, Regan MM, et al. External validation and comparison with other models of the International Metastatic Renal-Cell Carcinoma Database Consortium prognostic model: a population-based study. Lancet Oncol. 2013;14:141-8.
24. Gravallese EM, Schett G. Effects of the IL-23–IL-17 pathway on bone in spondyloarthritis. Nat Rev Rheumatol. 2018;14:631-40.
25. Dimitrov V, Bouttier M, Boukhaled G, et al. Hormonal vitamin D up-regulates tissue-specific PD-L1 and PD-L2 surface glycoprotein expression in humans but not mice. J Biol Chem. 2017;292:20657-68.
26. Pincikova T, Paquin-Proulx D, Sandberg J, Flodström-Tullberg M, Hjelte L. Vitamin D treatment modulates immune activation in cystic fibrosis. Clin Exp Immunol. 2017;189:359-71.
27. Borcherding N, Vishwakarma A, Voigt AP, et al. Mapping the immune environment in clear cell renal carcinoma by single-cell genomics. Commun Biol. 2021;4:1-11.
28. Nakano N, Nishiyama C, Kanada S, et al. Involvement of mast cells in IL-12/23 p40 production is essential for survival from polymicrobial infections. Blood. 2007;109:4846-55.
29. Shinagare AB, Vikram R, Jaffe C, et al. Radiogenomics of clear cell renal cell carcinoma: Preliminary findings of the cancer genome atlas–renal cell carcinoma (TCGA–RCC) imaging research group. Abdom imaging. 2015;40:1684-92.
30. Kocak B, Durmaz ES, Ates E, Ulusan MB. Radiogenomics in clear cell renal cell carcinoma: machine learning–based high-dimensional quantitative CT texture analysis in predicting PBRM1 mutation status. AJR Am J Roentgenol. 2019;212:W55-W63.

Corresponding Author:

Kewei Yang, MD;

Department of Radiology, Ningbo Urology and Nephrology Hospital, Ningbo 315000, China.

Tel: +86 574 55662503, Fax: +86 574 55662999, E-mail: syzdh_keweiyang@hotmail.com

Figure legends

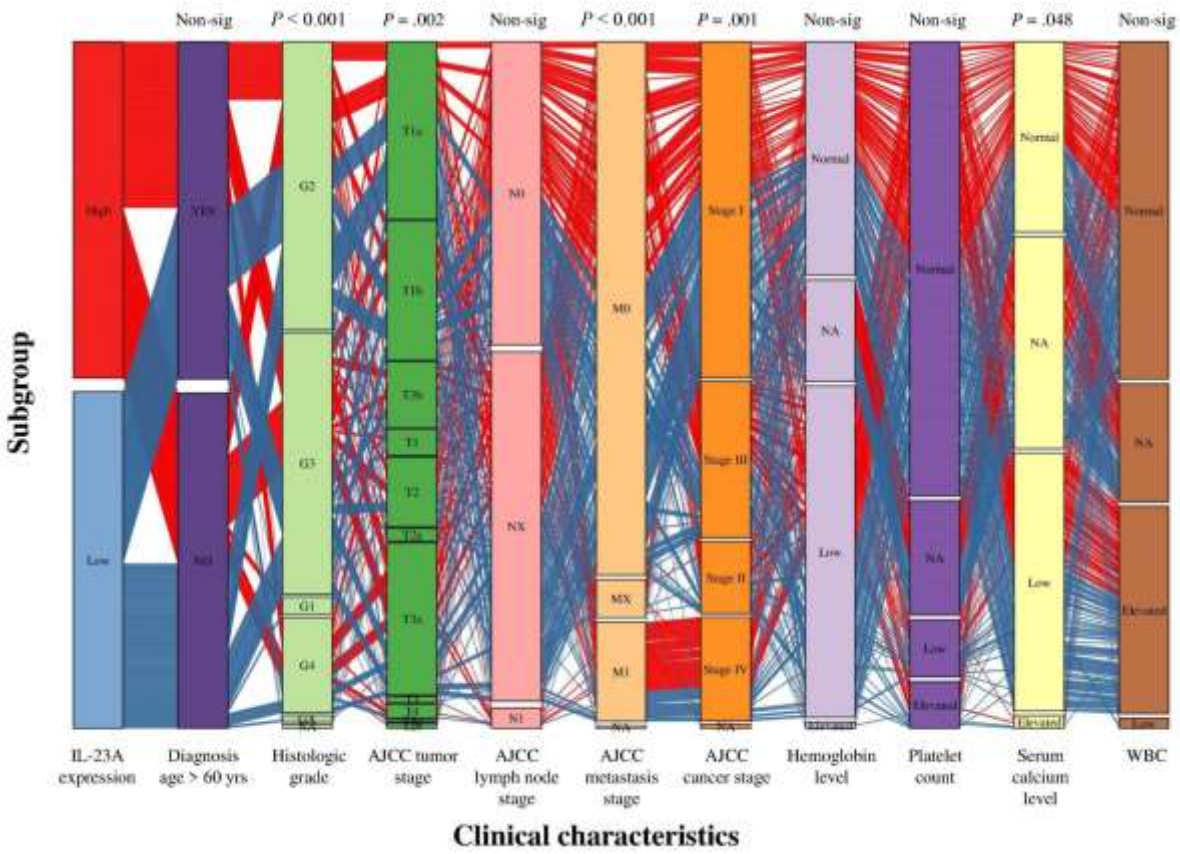

Figure 1. The Major clinical characteristics between IL-23 expression groups. Non-sig indicates no significance.

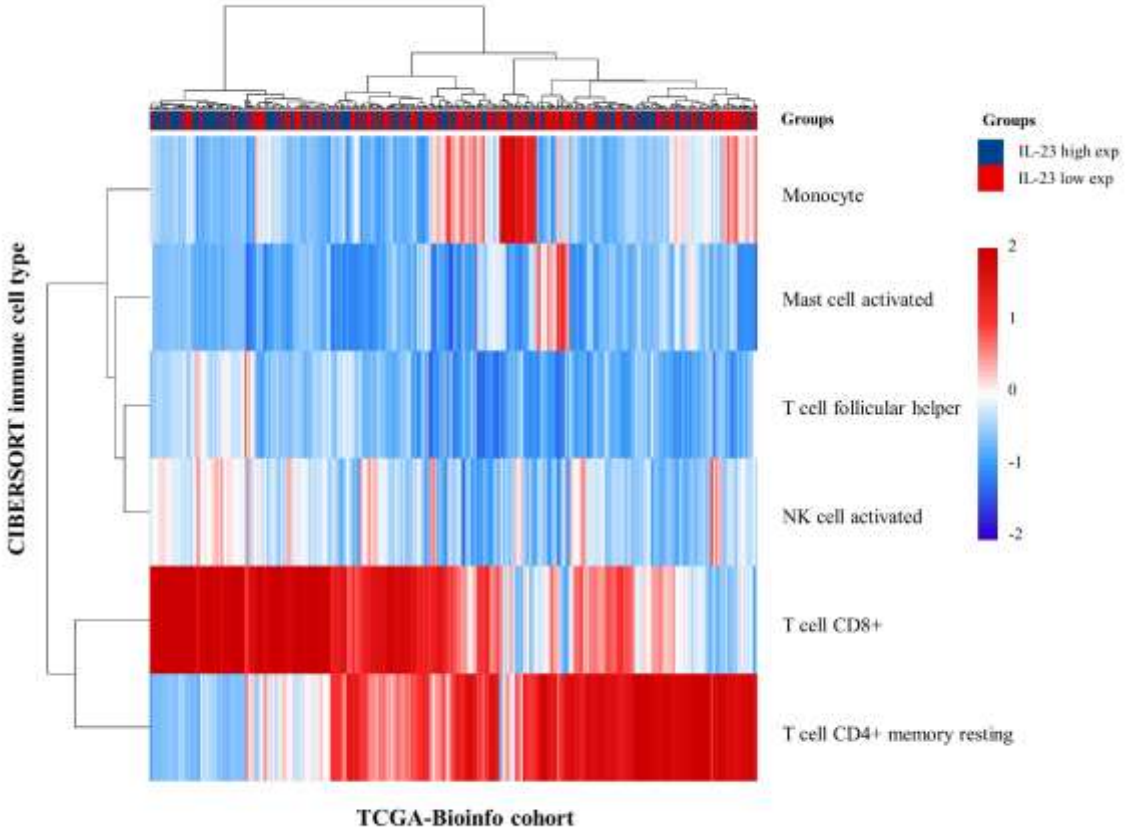

Figure 2. The immune cell infiltration status between IL-23 expression groups.

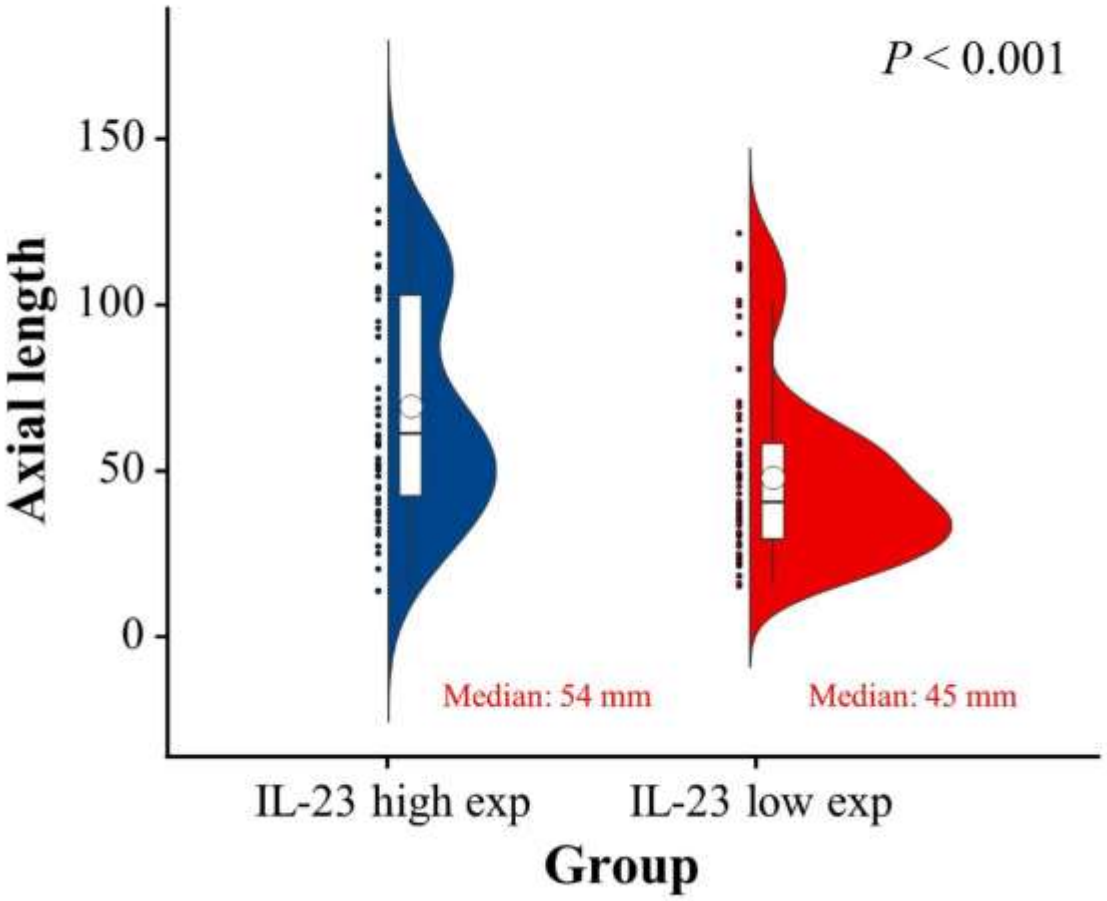

Figure 3. The axial length distribution between IL-23 expression groups.

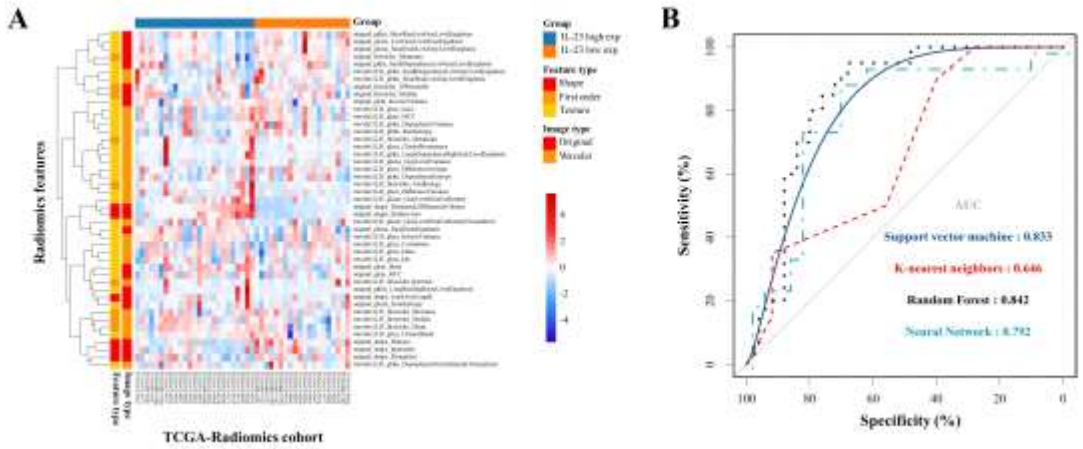

Figure 4. (A) The dimension reduced radiomics features of TCGA-Radiomics cohort. (B) The ROC curves of established IL-23 expression status prediction models.

Table 1. Cohort clinical characteristics. *missing data exists

Items	TCGA-Bioinfo (n=530)		TCGA-Radiographic (n=130)		TCGA-Radiomics (n=45)		*P-value: all cohorts*	*P-value: radiological cohorts*
	IL-23 high exp (n=265)	IL-23 low exp (n=265)	IL-23 high exp (n=60)	IL-23 low exp (n=70)	IL-23 high exp (n=25)	IL-23 low exp (n=20)		
Basic characteristics								
Sex: Female (case n)	92	94	25	17	13	9	0.13	0.047
Sex: Male (case n)	173	171	35	53	12	11		
Age at diagnosis (median; yrs)	60	61	60	58	62	58	0.53	0.74
Histologic grade*								
I/II (case n)	103	138	22	28	6	6	0.02	0.15
III/IV (case n)	161	120	38	42	19	14		
AJCC disease stage*								
I (case n)	111	154	23	43	8	9	0.16	0.26
II (case n)	30	27	6	3	1	1		
III (case n)	67	56	18	19	9	6		
IV (case n)	55	27	13	5	7	4		

Table 2. The IL-23 expression status predictive radiomics features

Feature name	Rank	Transformation	Subbands	Feature category	Information entropy gain
Maximum 2D Diameter Column	1	-	-	shape	0.489
Surface Area	2	-	-	shape	0.340
Total Energy	3	wavelet	LLH	first order	0.239
Gray Level Non Uniformity	4	wavelet	LLH	texture: glszm	0.212
Inverse Difference (Normalized)	5	wavelet	LLH	texture: glcm	0.164
Long Run High Gray Level Emphasis	6	-	-	texture: glrlm	0.160
Flatness	7	-	-	shape	0.149
Small Area Low Gray Level Emphasis	8	-	-	texture: glszm	0.141
Sphericity	9	-	-	shape	0.133
Inverse Difference Moment (Normalized)	10	-	-	texture: glcm	0.101
Inverse Variance	11	wavelet	LLH	texture: glcm	0.100
Low Gray Level Zone Emphasis	12	-	-	texture: glszm	0.093

Table 3. The confusion matrix of established machine learning models.

Machine learning algorithm	Actual IL-23 group		Sum
	high exp (n=25)	low exp (n=20)	
Random forest IL-23 group prediction			
High exp	21	6	27
Low exp	4	14	18
Support vector machine IL-23 group prediction			
High exp	20	6	26
Low exp	5	14	19
K-nearest neighbors IL-23 group prediction			
High exp	14	10	24
Low exp	11	10	21
Neural network IL-23 group prediction			
High exp	20	5	25
Low exp	5	15	20

Table 4. The prediction model performances

Machine learning algorithm	10-fold cross-validation			
	AUC (95% CI)	Accuracy	Sensitivity	Specificity
Random Forest	0.842 (0.648-0.927)	0.778	84.0%	70.0%
SVM	0.833 (0.679-0.920)	0.756	80.0%	70.0%
Neural Network	0.792 (0.675-0.917)	0.778	80.0%	75.0%
kNN	0.646 (0.509-0.799)	0.533	56.0%	50.0%